

# Journal of Biomedical Optics

[SPIDigitalLibrary.org/jbo](http://SPIDigitalLibrary.org/jbo)

## **Deep *in vivo* two-photon imaging of blood vessels with a new dye encapsulated in pluronic nanomicelles**

Mathieu Maurin  
Olivier Stéphan  
Jean-Claude Vial  
Seth R. Marder  
Boudewijn van der Sanden

# Deep *in vivo* two-photon imaging of blood vessels with a new dye encapsulated in pluronic nanomicelles

Mathieu Maurin,<sup>a</sup> Olivier Stéphan,<sup>a</sup> Jean-Claude Vial,<sup>a</sup> Seth R. Marder,<sup>b</sup> and Boudewijn van der Sanden<sup>c</sup>

<sup>a</sup>Laboratoire de Spectrométrie Physique, CNRS UMR 5588, 140 Avenue de la Physique, BP 87, 38402, Saint Martin d'Hères, France

<sup>b</sup>Georgia Institute of Technology, School of Chemistry and Biochemistry, and Center for Organic Electronics and Photonics, Atlantic Blvd., Atlanta, Georgia 30332-0400

<sup>c</sup>Institut des Neurosciences Grenoble, INSERM U836, Chemin Fortuné Ferrini, BP 170, 38042, La Tronche, Grenoble, 38042 France

**Abstract.** Our purpose is to test if Pluronic<sup>®</sup> fluorescent nanomicelles can be used for *in vivo* two-photon imaging of both the normal and the tumor vasculature. The nanomicelles were obtained after encapsulating a hydrophobic two-photon dye: di-styryl benzene derivative, in Pluronic block copolymers. Their performance with respect to imaging depth, blood plasma staining, and diffusion across the tumor vascular endothelium is compared to a classic blood pool dye Rhodamin B dextran (70 kDa) using two-photon microscopy. Pluronic nanomicelles show, like Rhodamin B dextran, a homogeneous blood plasma staining for at least 1 h after intravenous injection. Their two-photon imaging depth is similar in normal mouse brain, using 10 times less injected mass. In contrast with Rhodamin B dextran, no extravasation is observed in leaky tumor vessels due to their large size: 20–100 nm. In conclusion, Pluronic nanomicelles can be used as a blood pool dye, even in leaky tumor vessels. The use of Pluronic block copolymers is a valuable approach for encapsulating two-photon fluorescent dyes that are hydrophobic and not suitable for intravenous injection. © 2011 Society of Photo-Optical Instrumentation Engineers (SPIE). [DOI: 10.1117/1.3548879]

Keywords: intravital two-photon microscopy; cerebral and tumor microvasculature; pluronic nanomicelles.

Paper 10502RR received Sep. 14, 2010; revised manuscript received Dec. 17, 2010; accepted for publication Jan. 6, 2011; published online Mar. 1, 2011.

## 1 Introduction

Two-photon laser scanning microscopy (TPLSM) allows deep imaging (<1 mm) of biological tissues in living animals with a micrometric spatial resolution.<sup>1</sup> The observation depth depends, among other things, on tissue parameters, laser characteristics, optics, and finally, the physical-chemical properties of the fluorescent dye. Relevant fluorescent dyes for optical imaging are often hydrophobic and can therefore not be injected in animals. In the present study, a new approach of encapsulating hydrophobic two-photon dyes in Pluronic block copolymers was validated for two-photon imaging of the normal and the tumor vasculature in mice. In both cases, especially in the leaky vasculature of tumors, the nanomicelles should not diffuse across the vascular endothelium for proper detection of the local functional blood volume.<sup>2,3</sup> In other words, an enhanced permeability and retention effect is not desired during the measurements. This will overestimate the local blood volume and blur the two-photon images. This latter parameter is of crucial interest in biomedical applications such as tumor diagnosis and therapy follow-up.<sup>4</sup> Tumors have most often an abnormal vascular blood volume in comparison to normal adjacent tissue, which determines drug delivery and, consequently, their therapy response.

The new two-photon dyes should allow imaging at low laser power (<30 mW) at nontoxic concentrations without

modifying the blood viscosity. For TPLSM, main fluorescent dye specifications are: a high two-photon absorption cross section ( $\sigma_{TPA}$ ) and a fluorescence quantum yield  $\Phi$  with an emission and a two-photon absorption wavelength located in the spectral region of interest for bioimaging (680–1040 nm). Actually, regular intravascular dyes consist of branched polysaccharides (e.g., dextrans, grafted with organic dyes such as fluorescein or rhodamin).<sup>5,6</sup> Numerous other strategies use quantum dots,<sup>7</sup> water-soluble dendrimers,<sup>8</sup> or fluorescent dye-doped silica mesoporous nanoparticles.<sup>9</sup> Most of these particles are of limited use due to their *in vivo* instability or biotoxicity. Another approach involves nanodispersion of hydrophobic organic preformed compounds in aqueous solutions using special formulation techniques such as microemulsions.<sup>10</sup>

In this field, we recently reported the elaboration of organic fluorescent nanomicelles based on a microemulsion process using a well-known polyethylene–polypropylene glycol (Pluronic) surfactant.<sup>11</sup> This process leads to hydrophilic micelles encapsulating hydrophobic fluorescent molecules with dimensions ranging from 20 to 100 nm. This method can be applied to numerous hydrophobic dyes.<sup>12</sup> Here, a di-styryl benzene-modified derivative<sup>13</sup> has been used, exhibiting a 2500 GM ( $1 \text{ GM} = 10^{-50} \text{ cm}^4 \text{ s photon}^{-1} \text{ molecules}^{-1}$ ) two-photon absorption cross section at 800 nm. Its structure is shown in Fig. 1. To illustrate the potential for vasculature imaging of such probes, imaging of the cerebral vasculature has been performed in the cortex of normal mice. The maximum imaging depth and blood plasma staining have been compared to the regular blood pool

Address all correspondence to: Boudewijn van der Sanden, Institut des Neurosciences Grenoble, INSERM U836, Chemin Fortuné Ferrini, BP 170, 38042, La Tronche, Grenoble, 38042 France. Tel: 00 33 4 56 52 06 19; Fax: 00 33 4 56 52 06 39; E-mail: Boudewijn.vandersanden@ujf-grenoble.fr.

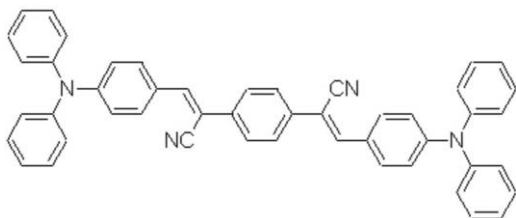


Fig. 1 Structure of the di-styrylbenzene derivative.

dye Rhodamin B Dextran (70 kDa). Quantitative blood volume measurement has been performed for both dyes and compared to values in the literature. Finally, the diffusion properties of the Pluronic nanomicelles has been analyzed and compared to those of Rhodamin B dextran, in the leaky tumor neovasculature of human lung carcinoma growing in dorsal skin-fold chambers.

## 2 Materials and Methods

### 2.1 Dyes Preparation

Pluronic F68 was purchased from Sigma-Aldrich (France). Synthesis of the di-styryl benzene derivative (Fig. 1) has already been reported.<sup>13</sup> For the Pluronic nanomicelles (Fig. 2), 2 mg of di-styryl benzene-modified derivative was dissolved in 100  $\mu\text{L}$  chloroform and added to 5 ml of Pluronic F68 (2 wt. %) aqueous solution containing 0.9% NaCl. After 15 min stirring for preemulsification, the microemulsion was prepared by ultrasonication for 15 min (bath, 150 W). After sonication, the mixture was stirred in a regulated bath at 50°C for 30 min to evaporate the chloroform. The colloidal particle size (20–100 nm) was fixed by mechanical filtration (Nylon-Cameo, Fisher, France) of the solution. Typically, dye concentrations, ranging from 0.1 to 0.15  $\text{g L}^{-1}$  (0.15 to 0.23  $\text{mmol L}^{-1}$ ), can be obtained in a 10  $\text{g L}^{-1}$  Pluronic aqueous solution.<sup>11</sup> As a reference, a 100  $\text{g L}^{-1}$  Rhodamin B dextran 70-kDa solution (Sigma-Aldrich, France) in 0.9% NaCl was prepared. Depending on the degree of Rhodamin B labeling of the dextran, the Rhodamin B dye concentrations varied between 4 and 11  $\text{mmol L}^{-1}$ .

### 2.2 Animal Models

Healthy Swiss white mice ( $n = 6$ , 6–8 weeks old) and tumor bearing Swiss nude mice ( $n = 3$ , 6 months old, Charles River Laboratories, Lyon, France) were used. All experiments were performed in accordance with the French Government guidelines (license A3851610008). During surgery and imaging, mice were anesthetized by a continuous inhalation of 2% isoflurane in a gas mixture of 30%  $\text{O}_2$  and 70%  $\text{N}_2\text{O}$ , and placed on a modified stereotaxic frame or on a homemade frame for proper fixation of mice with dorsal skin-fold chambers. Core temperature was maintained at  $\sim 37^\circ\text{C}$  using a warm water blanket. For the cerebral microvessel imaging experiments, a craniotomy ( $\phi = 3$  mm) was carried out above the left parietal cortex. A rubber ring was placed on the top of the skull to trap saline for continuous objective immersion.

For tumor vasculature imaging, three Swiss nude mice were implanted with small dorsal skin-fold chambers (small dorsal kit SM100, APJ Trading Company, Ventura, California) as described in a previous protocol.<sup>4</sup> Briefly, two symmetrical

titanium frames with central holes ( $\phi = 1$  cm) flanked the dorsal skin fold of animals sandwich the extended double layer of skin and create the dorsal skin-fold chamber, which consisted of one layer of striated muscle, s.c. tissue, and epidermis. An observation window, covered with a glass coverslip, allowed for intravital microscopic observations. One day after surgery, mice were checked on the presence of infection. At the absence of infection,  $2 \times 10^6$  human lung carcinoma cells (NCI-H460, ATCC No. HTB-177) in 200  $\mu\text{L}$  vehicle [50% RPMI medium, 50% matrigel (BD Matrigel TM Matrix No. 354234, Bedford, Massachusetts)] were injected in the dorsal skin-fold chamber. Two-photon imaging of the tumor vasculature was performed at 14 days after tumor cell injections.

For each experiment, 100  $\mu\text{L}$  of Pluronic microemulsion or Rhodamin B dextran solution in saline was injected in the tail vein of the mice  $\sim 1$  min before imaging.

### 2.3 Microscopy Set-up

*In vivo* two-photon laser scanning microscopy was performed with a confocal microscope consisting of a Biorad (MRC 1024) scanhead and an Olympus BX50WI microscope. A 800-nm excitation beam originating from a femtosecond Ti:sapphire laser (5-W pump; Spectra-Physics, Millennia V) was focused into the cortex using a 20 $\times$  water-immersion objective (0.95 numerical aperture, Xlum Plan FI Olympus). The laser beam was then scanned in the  $x$ - $y$  plane to acquire a 512  $\times$  512 image (0.9 s/image) with laser powers varying between 10 and 30 mW. The  $z$  scan (variation of the observation depth) was realized by translation of the motorized objective. For these experiments, the confocal configuration was not used and the non-descanned fluorescence was directly collected with an external photomultiplier protected by a BG39 filter (Schott Glass-Jena, Germany). Planar scans of the fluorescent intensity were acquired at successive depths in the animal with a 5- $\mu\text{m}$   $z$  step between scans. Image reconstruction and analysis were performed using free ImageJ software.<sup>14</sup>

### 2.4 Relative Blood Volume Measurement

Relative blood volume measurements (which equal total blood volume/total sample volume) have been performed using a method described by Verant et al.<sup>5</sup> For each stack, the background (rolling ball algorithm with a radius varying between 30 and 60  $\mu\text{m}$ ) and the saturated pixels due to artifacts are removed using ImageJ software. Per slice in a  $z$  stack, fluorescence intensities are normalized between 0 and 255 gray values using plunging vessels with maximum intensity (gray value 255). This is necessary to correct for the variation of fluorescence generation and collection as a function of depth. To finish, an average  $z$ -projection of the stack is performed. In this  $z$ -projection, the corresponding blood volume is proportional to the sum of the pixel intensities.

## 3 Results and Discussion

### 3.1 Cerebral Vasculature Imaging

Imaging of the cerebral vasculature in the cortex of normal Swiss white mice (6–8 weeks old) has been performed with Pluronic nanomicelles and Rhodamin B dextran. As shown in

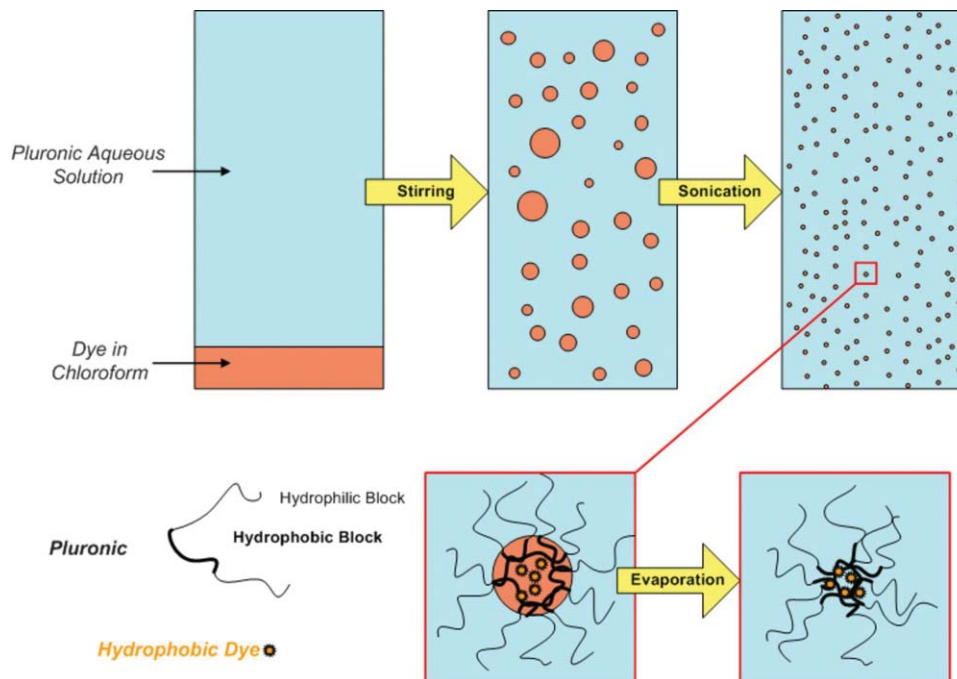


Fig. 2 Schematic representation of the Pluronic micelles synthesis (see text for details).

Fig. 3, vessels as far as 600  $\mu\text{m}$  below the dura were detected with both dyes. It is noted that two-photon optimized Pluronic nanomicelles exhibit the same efficiency when compared to Rhodamin B Dextran in spite of a ten times smaller mass. Minor effects on the blood viscosity and hemodynamics are expected after injection of Pluronic nanomicelles (100  $\mu\text{L}$  containing 1 mg Pluronic) in comparison to Dextran dyes (100  $\mu\text{L}$  containing 10 mg Dextran) without modifying the observation depth.

Ideally, blood dye concentration must be constant during the intravital microscopic studies, which take  $\sim 1$  h. Therefore, stacks were acquired every 10 min during 1 h after injection

of both dyes in different mice and the fluorescence intensity of specific vessels was quantified using ImageJ software (Fig. 4). For both dyes, it was noted that the fluorescence intensity is rather stable: 90% of the initial signal remained after 1 h. Thus, no important dye accumulation or clearance occurred within 1 h.

The stability of the Pluronic nanomicelles in blood was not investigated in detail.<sup>15</sup> The stability of the Pluronic nanomicelles depends on many physicochemical parameters that are unique for each encapsulated hydrophobic dye and Pluronic unimers. In the current study, our di-stryl benzene chromophore is known to aggregate in a hydrophobic environment. This

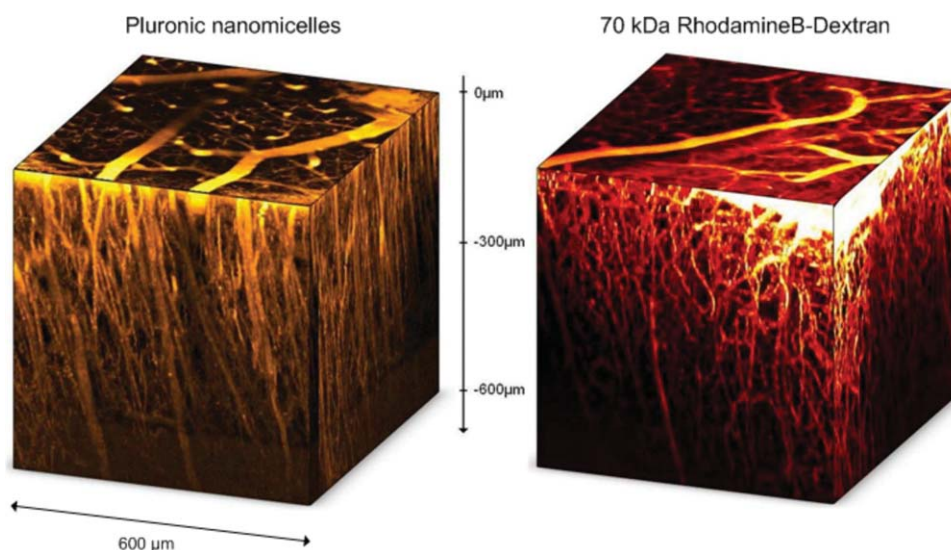
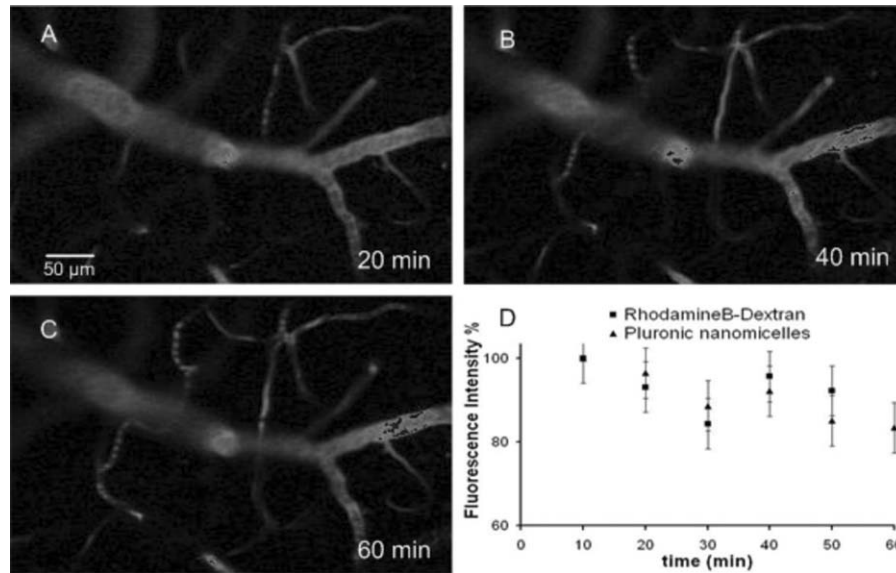
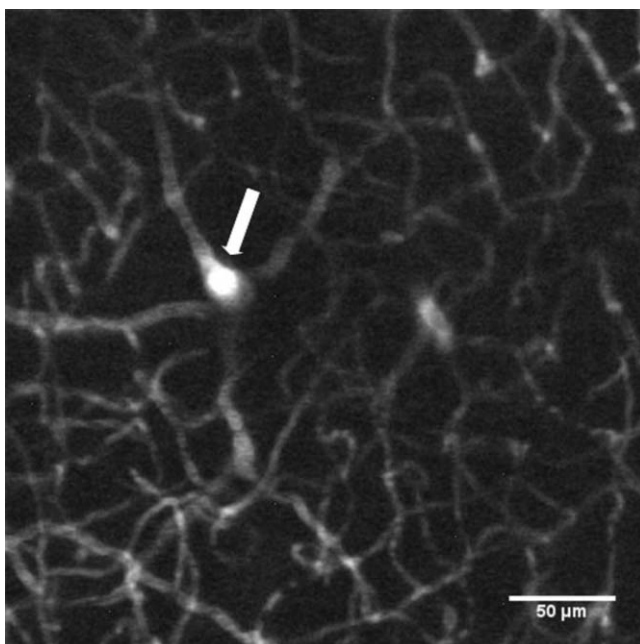


Fig. 3 Reconstructed 3-D data sets of z stacks ( $600 \times 600 \times 600 \mu\text{m}$ ) acquired below the dura in 120 steps of  $5 \mu\text{m}$  in the left parietal cortex of healthy Swiss white mice. Mice were injected with 100  $\mu\text{L}$  of  $100 \text{ g L}^{-1}$  Rhodamin B dextran or 100  $\mu\text{L}$  of  $10 \text{ g L}^{-1}$  Pluronic nanomicelles.



**Fig. 4** Images acquired at 150  $\mu\text{m}$  below the dura at (a) 20, (b) 40, and (c) 60 min after 100  $\mu\text{L}$  Pluronic nanomicelles ( $10 \text{ g L}^{-1}$ ) injection. (d) Decrease of the mean fluorescence signal intensity in all vessels (bars are SD) after injection of Pluronic nanomicelles or 70 kDa Rhodamin B dextran ( $100 \text{ g L}^{-1}$ ).

avored  $\pi$ - $\pi$  stacking and increased the two-photon absorption cross section.<sup>12</sup> This stacking of di-stryl benzene inside the hydrophobic core of the Pluronic nanomicelles might further increase their stability: a larger surface for hydrophobic interactions with the hydrophobic poly (propylene oxide) blocks. Binding of the aggregated di-stryl benzenes to hydrophobic



**Fig. 5** Z projection of the average fluorescence intensity of 41 images acquired from 100 to 300  $\mu\text{m}$  below the dura in the left parietal cortex of a Swiss white mouse after injection of 100  $\mu\text{L}$  of Pluronic nanomicelles ( $10 \text{ g L}^{-1}$ ). The plunging vessel (white arrow) is crucial for the normalization of the light intensity per slice.

components of the blood could not be excluded,<sup>15</sup> but might be retarded several hours.

### 3.2 Relative Cortical Blood Volume Measurements

Relative cortical blood volume (rCBV) measurements have been performed with previous stacks after Pluronic nanomicelles or Rhodamin B dextran injection using for both dyes three mice. For the relative blood volume calculations, the slices were taken at 50  $\mu\text{m}$  below the dura to suppress large superficial vessels of the subarachnoid space. An example of average z-projection of a specific area is shown in Fig. 5.

Using Pluronic nanomicelles, a rCBV of  $2.4 \pm 0.5$  (standard deviation)% was found, which was in good agreement with Rhodamin B dextran results: rCBV =  $2.3 \pm 0.3\%$ . Those results, close to the rCBV literature values,<sup>16</sup> demonstrate that our Pluronic nanomicelles are strictly plasmatic dyes.

### 3.3 Two-Photon Imaging of the Tumor Vasculature

In most high-grade tumors, the endothelium of new neovessels is often leaky for small molecules,<sup>17</sup> which leads to an higher interstitial fluid pressure.<sup>18,19</sup> For proper local tumor blood volume measurements, the dye should stay in the vasculature and not diffuse across the leaky endothelium. In the present study, we tested to see if Pluronic nanomicelles could be used as blood pool dyes in tumors and compared their performance to the Rhodamin B dextran 70 kDa dye. In Fig. 6, both dyes were injected with a 30-min interval in a mouse bearing a dorsal skinfold chamber with human lung carcinoma. The largest Pluronic nanomicelles were injected first and during 30 min, no dye diffusion across the vascular endothelium into the extravascular space was observed. The background between the vessels remained black and showed a good contrast with the functional

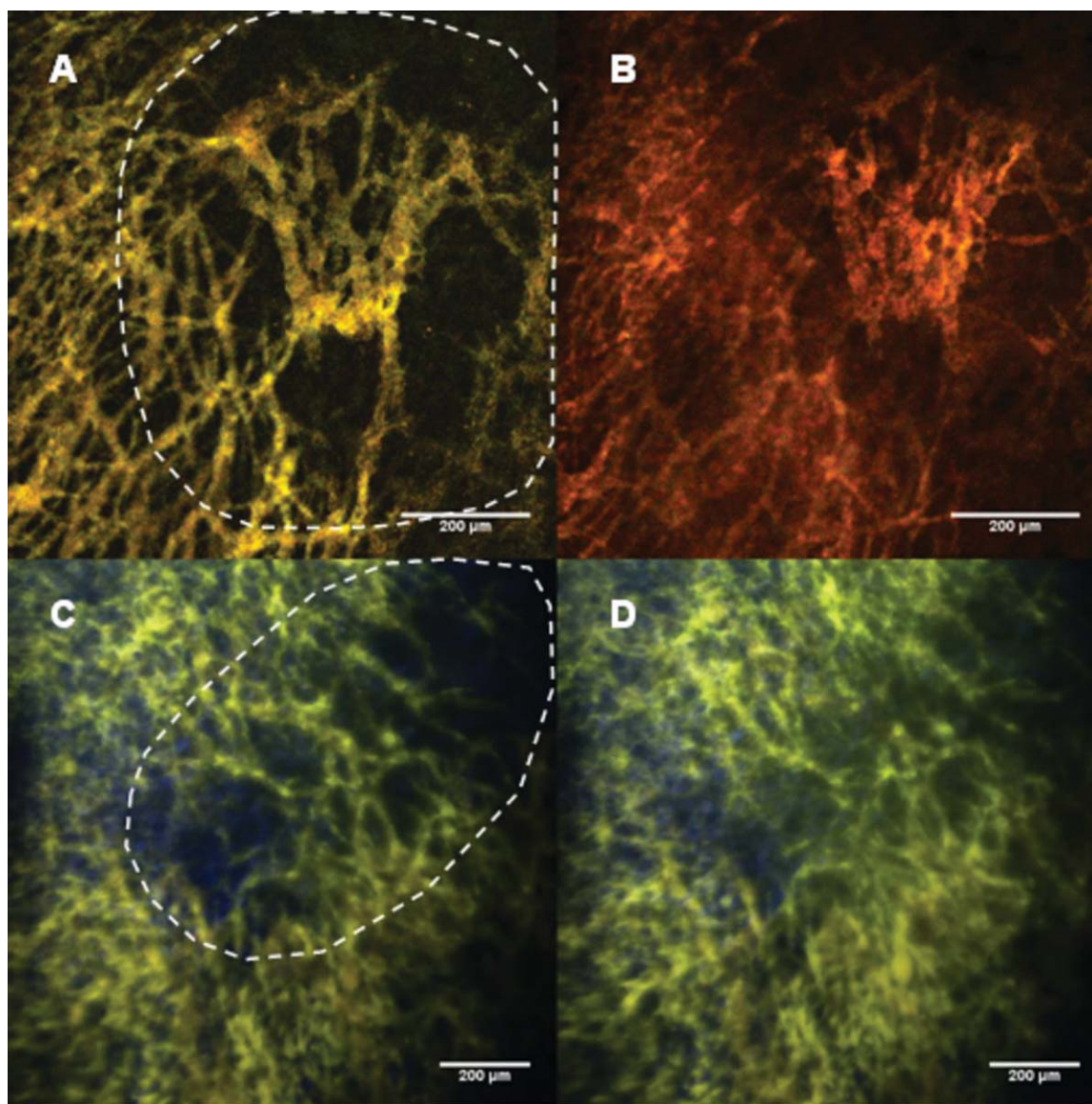


**Fig. 6** Images (size:  $848.53 \mu\text{m}^2$ ) of the tumor vasculature in Swiss nude mice bearing human lung carcinoma in a dorsal skin-fold chamber. The tumor areas are indicated by the dashed lines, and the length of the scale bars represent  $200 \mu\text{m}$ : (a) 30 min after  $100 \mu\text{L}$  of Pluronic nanomicelles ( $10 \text{ g L}^{-1}$ ) injection, (b) 30 min after a second injection of  $100 \mu\text{L}$  of 70 kDa Rhodamin B dextrans ( $100 \text{ g L}^{-1}$ ), and (c) z projection of average intensities in a stack of 40 images (thickness  $195 \mu\text{m}$ , image size:  $1214.56 \mu\text{m}^2$ ) of the tumor vasculature in another human lung carcinoma, after  $100 \mu\text{L}$  of Pluronic nanomicelles ( $10 \text{ g L}^{-1}$ ) injection at 1 min. after intraperitoneal (I.P.) injection of a vascular disrupting agent (VDA) and (d) 30 min after VDA treatment.

tumor vessels [Fig. 6(a)]. In a previous study, Pluronic nanomicelles were found to stay inside the tumor vasculature until 4 h after *i.v.* injection (results not shown).

Thirty minutes after the second injection of Rhodamin B dextran 70 kDa, the contrast between the vessels and the background got lost due to the diffusion of the Rhodamin B dextran dyes into the extravascular space [Fig. 6(b)]. This difference can be related to the important size of Pluronic nanomicelles (20–100 nm) in comparison to 70 kDa Rhodamin B dextran with a hydrodynamic radius of 6 nm. Even, the largest dextrans (200 kDa) with a hydrodynamic radius of 27 nm are known to diffuse across the leaky tumor blood vessels.<sup>17,18</sup> Note that at this molecular size, the solubility of the dextran decreases (maximum concentration 10 mg/ml) in comparison to the

70 kDa dextran (maximum concentration 100 mg/ml), which results in  $\sim 10$  times fewer dyes in the blood plasma.

The fast uptake of Pluronic nanomicelles could only be observed after treatment with a vascular disrupting agent that was known to drastically increase the vascular permeability [Figs. 6(c) and 6(d)].

#### 4 Conclusions

In the present study, we have demonstrated that Pluronic nanomicelles can be used as blood pool dyes in intravital two-photon imaging of both the normal and tumor vasculature. In the normal vasculature, the blood plasma staining is homogeneous and similar to the results obtained with the

Rhodamin B dextran at ten times less injected mass (1 mg Pluronic versus 10 mg 70 kDa grafted Dextran). In comparison to dextran dyes, minor effects on the blood viscosity and hemodynamics are expected with Pluronic nanomicelles. In a human lung carcinoma, Pluronic nanomicelles stayed in the vasculature, whereas Rhodamin B dextran diffused across the leaky tumor vascular endothelium. Therefore, Pluronic nanomicelles can be used for local tumor blood volume measurements during tumor growth and follow-up of antiangiogenic therapies. However, both the stability in blood and the toxicity of these nanomicelles have to be addressed first in a future study.

In general, the use of Pluronic block co-polymers is a valuable approach for encapsulating two-photon fluorescent dyes that are hydrophobic and not suitable for intravenous injection.

### Acknowledgments

This work was supported by a grant from the Ministère de l'Éducation Nationale, de l'Enseignement Supérieur et de la Recherche. The authors thank Patrice Baldeck for helpful discussion, and Cyril Zenga and Aurelie Juhem for biotechnical assistance in two-photon imaging of the tumor vasculature.

### References

1. W. Denk, J. H. Strickler, and W. W. Webb, "Two-photon laser scanning fluorescence microscopy," *Science* **248**(4951), 73–76 (1990).
2. B. D. Murphy, X. Chen, and T. Y. Lee, "Serial changes in CT cerebral blood volume and flow after 4 hours of middle cerebral occlusion in an animal model of embolic cerebral ischemia," *Am. J. Neuroradiol.* **28**(4), 743–749 (2007).
3. M. N. Sawka, V. A. Convertino, E. R. Eichner, S. M. Schnieder, and A. J. Young, "Blood volume: importance and adaptations to exercise training, environmental stresses, and trauma/sickness," *Med. Sci. Sports Exerc.* **32**(2), 332–348 (2000).
4. G. M. Tozer, S. M. Ameer-Beg, J. Baker, P. R. Barber, S. A. Hill, R. J. Hodgkiss, R. Locke, V. E. Prise, I. Wilson, and B. Vojnovic, "Intravital imaging of tumour vascular networks using multi-photon fluorescence microscopy," *Adv. Drug Del. Rev.* **57**(1), 135–152 (2005).
5. P. Verant, R. Serduc, B. Van Der Sanden, C. Remy, and J. C. Vial, "A direct method for measuring mouse capillary cortical blood volume using multiphoton laser scanning microscopy," *J. Cereb. Blood Flow Metab.* **27**(5), 1072–1081 (2007).
6. K. Andrieux, P. Lesieur, S. Lesieur, M. Ollivon, and C. Grabielle-Madelmont, "Characterization of fluorescein isothiocyanate-dextran used in vesicle permeability studies," *Anal. Chem.* **74**(20), 5217–5226 (2002).
7. D. R. Larson, W. R. Zipfel, R. M. Williams, S. W. Clark, M. P. Bruchez, F. W. Wise, and W. W. Webb, "Water-soluble quantum dots for multiphoton fluorescence imaging *in vivo*," *Science* **300**(5624), 1434–1436 (2003).
8. T. R. Krishna, M. Parent, M. H. V. Werts, L. Moreaux, S. Gmouh, S. Charpak, A. M. Caminade, J. P. Majoral, and M. Blanchard-Desce, "Water-soluble dendrimeric two-photon tracers for *in vivo* imaging," *Angew. Chem.-Int. Ed.* **45**(28), 4645–4648 (2006).
9. V. Lebreton, L. Raehm, J. O. Durand, M. Smaïhi, C. Gerardin, N. Nerambourg, M. H. V. Werts, and M. Blanchard-Desce, "Synthesis and characterization of fluorescently doped mesoporous nanoparticles for two-photon excitation," *Chem. Mater.* **20**(6), 2174–2183 (2008).
10. D. Horn and J. Rieger, "Organic nanoparticles in the aqueous phase—theory, experiment, and use," *Angew. Chem.-Int. Ed.* **40**(23), 4331–4361 (2001).
11. M. Maurin, L. Vurth, J. C. Vial, P. Baldeck, S. R. Marder, B. Van Der Sanden, and O. Stephan, "Fluorescent Pluronic nanodots for *in vivo* two-photon imaging," *Nanotechnology* **20**(23), 235102 (2009).
12. M. Maurin, L. Vurth, J. C. Vial, P. Baldeck, S. R. Marder, B. Van Der Sanden, and O. Stéphan, "Pluronic organic fluorescent probes for two-photon vascularisation imaging," *Nonlinear Opt., Quantum Opt.: Concepts Mod. Opt.* **40**(1–4), 175–181 (2010).
13. S. J. K. Pond, M. Rumi, M. D. Levin, T. C. Parker, D. Beljonne, M. W. Day, J.-L. Bredas, S. R. Marder, and J. W. Perry, "One- and two-photon spectroscopy of donor-acceptor-donor distyrylbenzene derivatives: effect of cyano substitution and distortion from planarity," *J. Phys. Chem. A* **106**(47), 11470–11480 (2002).
14. Web site for free ImageJ software+ plugins downloads: <http://rsbweb.nih.gov/ij/>.
15. H. Chen, S. Kim, W. He, H. Wang, P. S. Low, K. Park, and J. X. Cheng, "Fast release of lipophilic agents from circulating PEG-PDLLA micelles revealed by *in vivo* forster resonance energy transfer imaging," *Langmuir* **24**(10), 5213–5217 (2008).
16. P. S. Tsai, J. P. Kaufhold, P. Blinder, B. Friedman, P. J. Drew, H. J. Karten, P. D. Lyden, and D. Kleinfeld, "Correlations of neuronal and microvascular densities in murine cortex revealed by direct counting and colocalization of nuclei and vessels," *J. Neurosci.* **29**(46), 14553–14570 (2009).
17. H. F. Dvorak, J. A. Nagy, J. T. Dvorak, and A. M. Dvorak, "Identification and characterization of the blood vessels of solid tumors that are leaky to circulating macromolecules," *Am. J. Pathol.* **133**(1), 95–109 (1988).
18. R. K. Jain, "Transport of molecules across tumor vasculature," *Cancer Metastasis Rev.* **6**(4), 559–593 (1987).
19. M. Leunig, F. Yuan, M. D. Menger, Y. Boucher, A. E. Goetz, K. Messmer, and R. K. Jain, "Angiogenesis, microvascular architecture, microhemodynamics, and interstitial fluid pressure during early growth of human adenocarcinoma LS174T in SCID mice," *Cancer Res.* **52**(23), 6553–6560 (1992).